An intractable climate archive -- Sclerochronological and shell oxygen isotope analyses of the Pacific geoduck, Panopea abrupta (bivalve mollusk) from Protection Island (Washington...

ARTICLE *in* PALAEOGEOGRAPHY PALAEOCLIMATOLOGY PALAEOECOLOGY · NOVEMBER 2008

Impact Factor: 2.34 · DOI: 10.1016/j.palaeo.2008.08.010

Palaeogeography, Palaeoclimatology, Palaeoecology 269 (2008) 115–126

Contents lists available at ScienceDirect

Palaeogeography, Palaeoclimatology, Palaeoecology

journal homepage: www.elsevier.com/locate/palaeo

An intractable climate archive — Sclerochronological and shell oxygen isotope analyses of the Pacific geoduck, *Panopea abrupta* (bivalve mollusk) from Protection Island (Washington State, USA)

Nadine Hallmann [a], Bernd R. Schöne [a,*], Are Strom [b], Jens Fiebig [c]

[a] *Department of Applied and Analytical Paleontology and INCREMENTS Research Group, Institute of Geosciences, University of Mainz, Johann-Joachim-Becher-Weg 21, 55128 Mainz, Germany*
[b] *WDFW Point Whitney Shellfish Lab, 1000 Point Whitney Rd., Brinnon, WA. 98320, USA*
[c] *Department of Paleontology, Institute of Geosciences, University of Frankfurt, Altenhöferallee 1, 60438 Frankfurt, Germany*

ARTICLE INFO

Article history:
Received 6 February 2008
Received in revised form 28 July 2008
Accepted 13 August 2008

Keywords:
Temperature
Bivalve
Oxygen isotopes
Disequilibrium fractionation
Climate
North Pacific

ABSTRACT

Annual growth increment patterns of cardinal teeth (CT) of *Panopea abrupta* (Conrad) can reportedly provide information about past climate variations. However, little is known about the intra-annual timing and rate of shell growth necessary to interpret such records. In addition, it remains unclear whether actual temperatures can be reliably inferred from $\delta^{18}O$ values of geoduck {goo'e-duk} shells. This study compared high-resolution environmental records (hourly to monthly resolved temperature, bi-weekly to monthly $\delta^{18}O_{water}$ and salinity data) with temperatures reconstructed from oxygen isotope values of the outer shell layer ($T\delta^{18}O_{OSL}$) and cardinal tooth portions ($T\delta^{18}O_{CT}$) of different contemporaneous specimens alive at the same locality. Results indicate that shell growth mainly occurred between March/April and November/December with a maximum during May–August. This finding must be considered when comparing the "annual" growth increment width chronologies to environmental parameters. In addition, intra-annual $\delta^{18}O_{shell}$ values require the calculation of weighted averages instead of arithmetic means. During ontogeny, the duration of the growing season remained nearly unchanged; an important finding for paleoclimate studies based on inter-annual growth patterns. Seasonal shell growth was strongly correlated with temperature (R=0.93, R^2=0.86, $p<0.0001$). Presumably due to individual differences in the exchange rate between the extrapallial fluid (EPF) and the ambient water, the outer shell layer of some specimens formed out of oxygen isotopic equilibrium, particularly during summer (high growth rates, increased ^{18}O depletion of the EPF). This resulted in a $T\delta^{18}O_{OSL}$ difference of up to 2 °C among different specimens. In addition, a bias was observed in different specimens toward daytime or nighttime temperatures, particularly during summer. Such a bias may be related to individual differences in the physiological activity at ultradian time-scales or to elevated predation pressure. More importantly, CT portions (= inner shell layer) formed in isotopic disequilibrium with the ambient water. Typically, reconstructed temperatures differed by more than 3–4 °C from actual water temperatures. Within specimens, $T\delta^{18}O_{OSL}$ and $T\delta^{18}O_{CT}$ were offset by ca. 2 °C. Some $T\delta^{18}O_{CT}$ also exhibited unexplained inter-annual trends, so that $T\delta^{18}O_{CT}$ among specimens varied by up to 4 °C. Given the $\delta^{18}O_{shell}$ inconsistency between and among shells, a small seasonal temperature amplitude barely exceeding 4 °C and the error bars of $T_{\delta 18O}$ of geoducks at this setting on the order of ±2 °C (error bars of the paleothermometry equation + variable $\delta^{18}O_{water}$ values + precision error of the mass spectrometer), the geochemical record of a single *P. abrupta* may not serve as a suitable paleoclimate archive. A reliable approximation to paleotemperatures may only be achieved by exclusively sampling the outer shell layer of multiple contemporaneous specimens, so that the $T\delta^{18}O_{OSL}$ variance among shells can be quantified.

1. Introduction

Skeletons of many aquatic organisms function as recorders of environmental and climate change. Particularly, long-lived bivalve mollusks such as *Arctica islandica* (Linnaeus), *Cucullaea raea* Zinsmeister, *Margaritifera margaritifera* (Linnaeus), or *Panopea abrupta* (Conrad) are increasingly used to reconstruct climate variations prior to anthropogenic forcing in the North Atlantic or North Pacific, respectively (Marchitto et al., 2000; Schöne et al., 2003; Buick and Ivany, 2004; Schöne et al., 2004a,b; Strom et al., 2004; Schöne et al., 2005a; Strom et al., 2005; Wanamaker et al., 2007). Such data is relevant because knowledge of natural low frequency climate oscillations (e.g., the Pacific Decadal Oscillation, PDO, or the El Niño/

* Corresponding author.
E-mail address: schoeneb@uni-mainz.de (B.R. Schöne).

0031-0182/$ – see front matter © 2008 Elsevier B.V. All rights reserved.
doi:10.1016/j.palaeo.2008.08.010

Southern Oscillation, ENSO) prior to the extensive anthropogenic forcing is needed to test and validate climate models. The interest in using bivalve sclerochronology s.l. (analyses of growth patterns, crystallography and geochemistry) for paleoclimate analyses partly results from significantly improved microanalytical techniques (e.g., micromilling: Dettman and Lohmann, 1995; mass spectrometry: Spötl and Vennemann, 2003; Fiebig et al., 2005), but also from the recognition that mollusks provide several advantages over other environmental and climate proxy archives. Bivalves form their valves by periodic accretion of skeletal hard parts, analogous to annual growth bands in corals (Hudson et al., 1976; Dodge and Vaišnys, 1980) or tree rings (Fritts, 1972). In addition, they inhabit nearly every aquatic environment. Thus, bivalve sclerochronology can potentially link proxy records from different settings, for example, high-latitude dendrochronology and tropical coral sclerochronology. Some bivalve species grow shell carbonate uninterruptedly for several centuries permitting the reconstruction of quasi- and multi-decadal climate oscillations (Schöne et al., 2003; Strom et al., 2004; Wanamaker et al., 2007). During growth, bivalve mollusks faithfully archive environmental changes in their skeletons in the form of variable growth rates and variable geochemical properties (e.g. Epstein et al., 1953; Jones et al., 1989; Goodwin et al., 2001; Surge and Walker, 2006). Furthermore, shell growth patterns function as a calendar that places the environmental proxy record in a temporal context (Clark, 1975; Jones, 1980; Johnson et al., 2000; Elliot et al., 2003).

However, a reliable interpretation of proxy records acquired from mollusk shells first and foremost requires precise knowledge of the timing and rate of biomineralization during different seasons. Typically, shells grow faster at warmer temperatures and when food supply is higher (e.g. Henderson, 1929; Kennish and Olsson, 1975; Page and Hubbard, 1987; Sato, 1997). Therefore, powder samples taken from these shells at equidistant spatial intervals typically represent different amounts of time. Shell portions near the annual growth lines grew slower, whereas those from about half-way between two consecutive growth lines were deposited in shorter time intervals. Consequently, calculation of annual averages from such samples requires weighted averaging (Schöne et al., 2005b). Furthermore, individual differences in the response to environmental forcings are likely to exist. Gillikin et al. (2005) noted a $\delta^{18}O$ difference of up to 0.2‰ in three contemporaneous shells of *Saxidomus giganteus* (DeShayes) from the same habitat indicating that a single specimen may not be sufficient to reliably reconstruct the climate of the past.

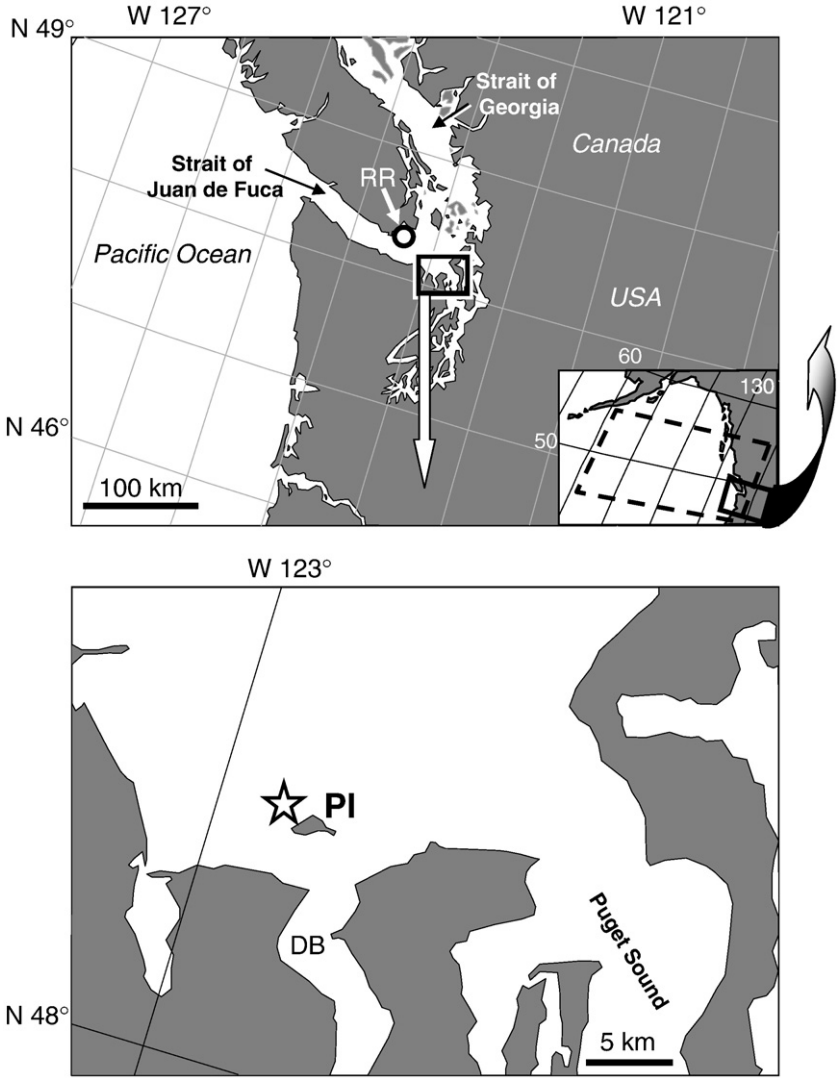

Fig. 1. Map showing the sample locality (star in lower panel) of the *Panopea abrupta* specimens (Table 1) and water samples (Table 2) NW of Protection Island (PI) near Discovery Bay (DB). Two temperature loggers were deployed at PI as well. Additional salinity data came from Race Rocks (RR) and were used to calculate $\delta^{18}O_{water,\ reco}$ values. The rectangle in the small map of the upper panel indicates the data grid of the $\delta^{18}O_{water}$ and salinity values that were used to calculate the freshwater mixing line and the region of the $SST_{satellite}$ data used to reconstruct bottom water temperatures from shell oxygen isotopes and salinity (Table 2) at PI.

Table 1
List of *Panopea abrupta* specimens used in this study

Specimen	Date of collection	Ontogenetic age (yr)	Ventral margin thickness (mm)	$\delta^{18}O_{shell}$ analysis (number of samples, time interval, shell portion)
AS-Mar-A1L	28 Mar 2005	6	0.83	70, 1999–March 2004, CT
AS-Apr-A1L	8 April 2005	6	0.63	108, January 2004–April 2005, OSL
… — A1R				27, 1999–April 2004, CT
AS-0806-A1L	18 Aug 2006	73	2.00	
AS-0806-A2L	18 Aug 2006	25	1.60	27, April 2005–August 2006, OSL
AS-0806-A3L	18 Aug 2006	41	1.33	
AS-0806-A4L	18 Aug 2006	63	2.23	
AS-0806-A5L	18 Aug 2006	41	1.64	
AS-0806-A6R	18 Aug 2006	16	1.67	46, September 2004–August2006, OSL
AS-0806-A7L	18 Aug 2006	71	2.00	
AS-0806-A8L	18 Aug 2006	62	1.84	

Four shells were isotopically analyzed.

Finally, it is necessary to know which portions of the shell are suitable geochemical proxy archives of climate change. For example, previous studies reported significant differences in trace element and stable isotope composition in the inner and outer shell layers (Gillikin et al., 2005; Surge and Walker, 2006). Therefore, life history traits and the basic mechanisms of shell deposition are prerequisite for a state-of-the-art sclerochronology-based paleoclimate analysis.

Here, we studied the growth patterns and oxygen isotope geochemistry of shells of the bivalve mollusk *P. abrupta* from the Northwest Pacific. Our primary goals were to identify the average duration of the growing season and variable rates of shell formation during different seasons. In addition, we asked the following questions: (1) Do shell $\delta^{18}O$ values of this species provide reliable temperature estimates; (2) If so, do such records differ among specimens; (3) Which shell portions are suitable for shell growth and isotope analyses, the cardinal tooth (inner shell layer) or the outer shell layer? Results of the present study are indispensable to properly utilize the Pacific geoduck as a paleoclimate proxy archive.

2. Materials and methods

Ten shells of *Panopea abrupta* were collected alive during 2005 and 2006 from a subtidal tract west of Protection Island (N48°08.4, W122°57; water depth of ca. 14 m) near the mouth of Discovery Bay in the Strait of Juan de Fuca, Washington State, USA (Fig. 1, Table 1). Shells lived ca. 70–100 cm below the sediment water interface. The Strait of Juan de Fuca lies between the Pacific Ocean and Puget Sound and the Strait of Georgia (Fig. 1). This passage is characterized by strong currents and an intense tidal mixing which results in relatively constant water temperatures and an unstratified surface water body (Mackas and Harrison, 1997). Growth of bivalve shells from Protection Island such as *P. abrupta* is thus strongly linked to sea surface temperatures (SST) (Strom et al., 2005).

2.1. Geoducks — bivalve(d) Methuselahs

The Pacific geoduck {goo'e-duk}, *P. abrupta* (Fig. 2), is extremely long-lived and reaches a lifespan of up to 160 yr (Bureau et al., 2002; Strom et al., 2004). Each year a sharply delimited growth line is deposited in the cardinal tooth (Fig. 3A) enabling a reliable estimate of ontogenetic ages of the shells (Shaul and Goodwin, 1982; Strom et al., 2004, 2005; Goman et al., 2007). Variations in annual shell growth reflect climate and environmental fluctuations (Strom et al., 2004). Geoducks were first identified as a potential climate proxy by Noakes and Campbell (1992). These authors postulated that shell growth co-varies with temperature. Modified dendrochronological methods were then applied to retrieve temperature estimates from geoducks (Strom et al., 2004). *P. abrupta* is broadly distributed in shallow waters in the entire North Pacific

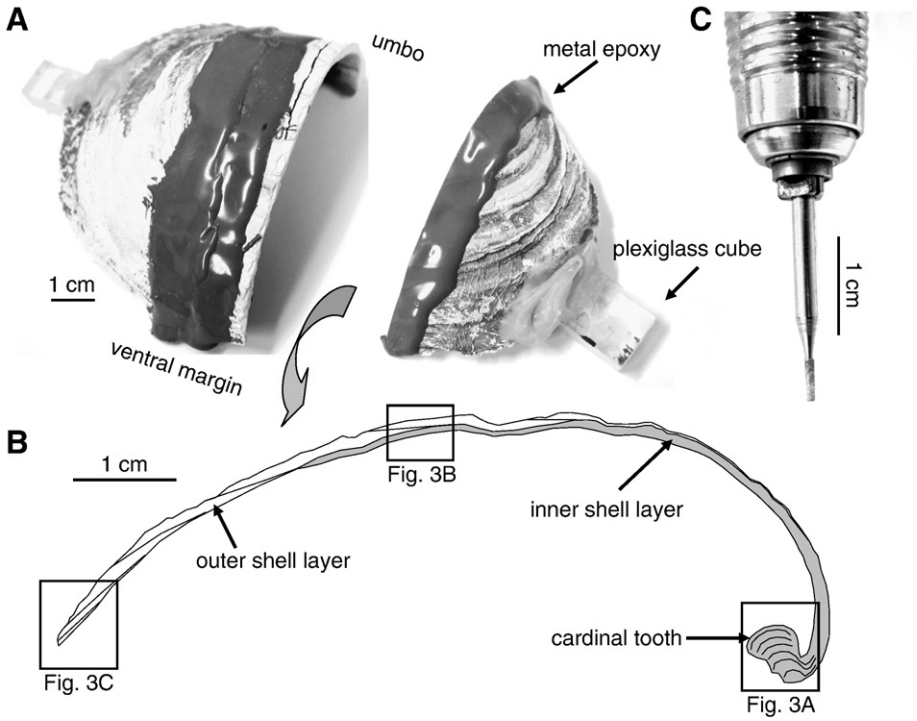

Fig. 2. Sample preparation of *Panopea abrupta* shells. (A) The shell was mounted on a plexiglass block, covered with metal epoxy and cut along the height axis perpendicular to the growth lines. Two immediately adjacent slabs (2–3 mm thick) were then mounted on glass slides. (B) Typical cross-section of the shells depicting the outer and inner shell layer (including the cardinal tooth) that were precipitated by the outer and inner extrapallial fluid, respectively. (C) Micromilling equipment that was used to obtain powder samples from the shells for stable isotope analyses.

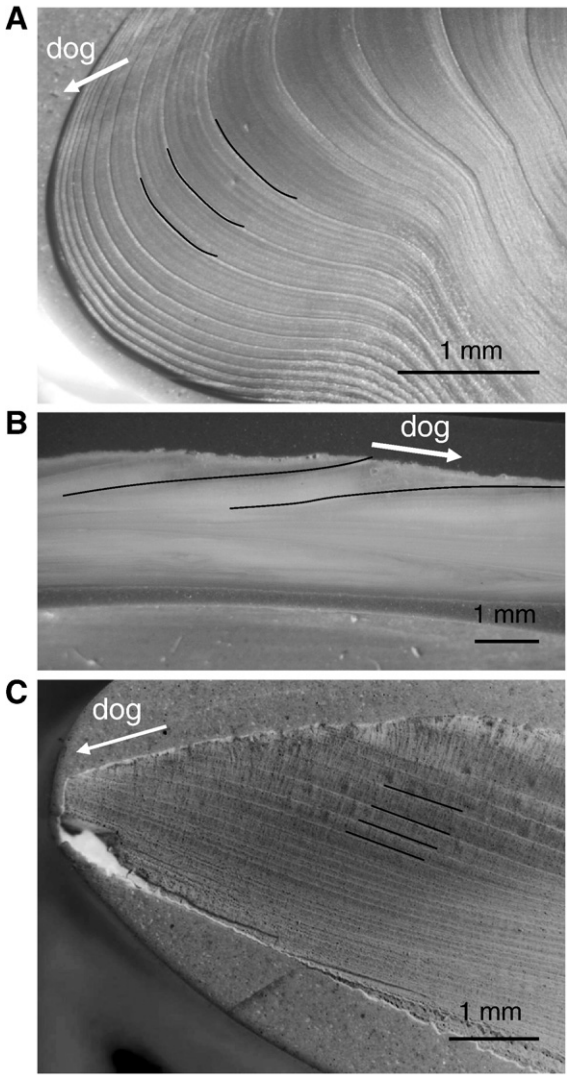

Fig. 3. When viewed under a binocular microscope, cross-sections of *Panopea abrupta* shells immersed in Mutvei's solution reveal annual growth patterns. These consist of distinct growth lines (black lines) that delimit growth increments and are best viewed in the cardinal tooth portion (A). (B and C) In the outer shell layer, these growth patterns are less well developed and difficult to recognize. (B) About half-way between the umbo (A) and the ventral margin (C) annual growth lines approach the outer shell surface at an angle of about 10° suggesting that the shell was growing rapidly in size. dog = direction of growth.

(Goodwin and Pease, 1989). This subtidal, infaunal suspension feeder occurs in marine and estuarine waters at depths of over 110 m from Alaska to Baja California, along the west coast of North America, around Japan (Goodwin and Pease, 1989) and New Zealand (Gribben and Creese, 2003) as well as in the South Atlantic (Morsán and Ciocco, 2004). In Japan and the American Northwest, *Panopea* sp. is commercially harvested and considered a delicacy. The geographic center of geoducks' distribution, however, is Puget Sound, USA and British Columbia, Canada. Preferentially, *P. abrupta* lives in soft substrates such as mud and sand, but also in pea gravel or gravel substrates and mixtures of these. As shown by mark-and-recovery experiments, geoducks in Puget Sound grow primarily from March through October (Shaul and Goodwin, 1982; Strom et al., 2004) and reproduce from April to July with peaks in May and June (Goodwin, 1976).

2.2. Preparation

For sclerochronological and isotope analyses, the ten studied shells (Table 1) were mounted on plexiglass cubes with plastic welder (Multipower, GlueTec). Preparation and analytical steps are shown in Fig. 2. After coating with metal epoxy resin (WIKO), the shells were cut perpendicular to the axis of growth along the shell height axis from the umbo to the ventral margin (Fig. 2A) using a low-speed precision saw (Buehler, IsoMet 1000) and 0.4 mm thick diamond-coated saw blades. Two sections of each valve were mounted on glass slides. In order to visualize the internal growth patterns (Fig. 3), the radial cross-sections (Fig. 2B) were ground on glass plates (800, 1200 grit powder) and polished with 1 μm Al_2O_2 powder. After each step, the valves were ultrasonically rinsed in de-ionized water to remove any adhering grinding powder from the shells.

2.3. Shell growth patterns

For sclerochronological analyses, one polished section of each specimen was cleaned with water-free ethanol and immersed in Mutvei's solution for 20 min under constant stirring at 37 °C to 40 °C (Schöne et al., 2005c). Stained sections were then carefully rinsed with de-ionized water and air-dried. Immersion in Mutvei's solution gently etches the carbonate and differentially stains the glycoproteins of the biominerals (Schöne et al., 2005c). Etch-resistant, organic-rich growth lines (dark blue) and stronger etched growth increments (light blue) can now easily be identified (Fig. 3).

Digital images of the growth patterns were taken from the umbonal shell regions (Fig. 3A) and from the outer shell layer approx. half-way between the umbo and the commissure (Fig. 3B) and from the ventral margin (Fig. 3C) with a Nikon Coolpix 995 camera attached to a binocular microscope (Wild Heerbrugg M3Z). Subsequently, the widths of the growth increments were measured in the direction of growth to the nearest 8 μm using the image analysis software Panopea (© Peinl and Schöne). Ontogenetic age and annual increment widths (Shaul and Goodwin, 1982) were determined by counting and measuring the distance between major growth lines. The ventral margin thickness was measured 2–7 mm away from the ventral margin (Table 1).

2.4. Oxygen isotope analyses

For the analysis of the oxygen isotope values of the shells, $\delta^{18}O_{shell}$, powder samples were taken from the remaining polished cross-sections of four bivalves (Fig. 3A and C). We sampled the outer shell layer near the ventral margin ($\delta^{18}O_{OSL}$) of three individuals and the cardinal tooth sections ($\delta^{18}O_{CT}$) of two specimens (Figs. 4–7). Ontogenetic ages of the sampled specimens ranged from six to 25 yr (Table 1). Prior to sampling, the slabs were ultrasonically rinsed in de-ionized water. Shell powder samples were obtained by milling parallel to the growth lines and perpendicular to the direction of growth with a cylindrical drill bit (1 mm diameter, Komet/Gebr. Brasseler GmbH & Co. KG, model no. 835 104 010; Figs. 2C and 3A and C). Samples were taken from the growing edge back toward youth portions of the shells. Each sample represents spatially equidistant shell portions ranging from 13 to 21 μm in the outer shell layer and ca. 60 to 120 μm in the cardinal teeth. Each powder sample weighed between 40 and 130 μg. Samples were processed in a Thermo Finnigan MAT 253 isotope ratio mass spectrometer equipped with a Gas Bench II following the method described by Spötl and Vennemann (2003). Results are reported in the usual δ-notation. The samples were measured against the NBS-19 calibrated Carrara marble standard ($\delta^{18}O = -1.74‰$). Per day, we measured 52 shell carbonate samples and 12 Carrara marble standards. Four Carrara standards were placed at the beginning of each daily run, after 24 shell samples and at the end of the remaining 28 samples. On average, the 1σ error of each shell carbonate analyses was better than 0.06‰. The $\delta^{18}O$ values of the shells ($\delta^{18}O_{shell}$) were calculated against the VPDB (Vienna Pee Dee Belemnite) standard and expressed as parts per mil.

If the oxygen isotopy of the water ($\delta^{18}O_{water}$) is known, $\delta^{18}O_{shell}$ values can provide detailed information on the ambient temperature

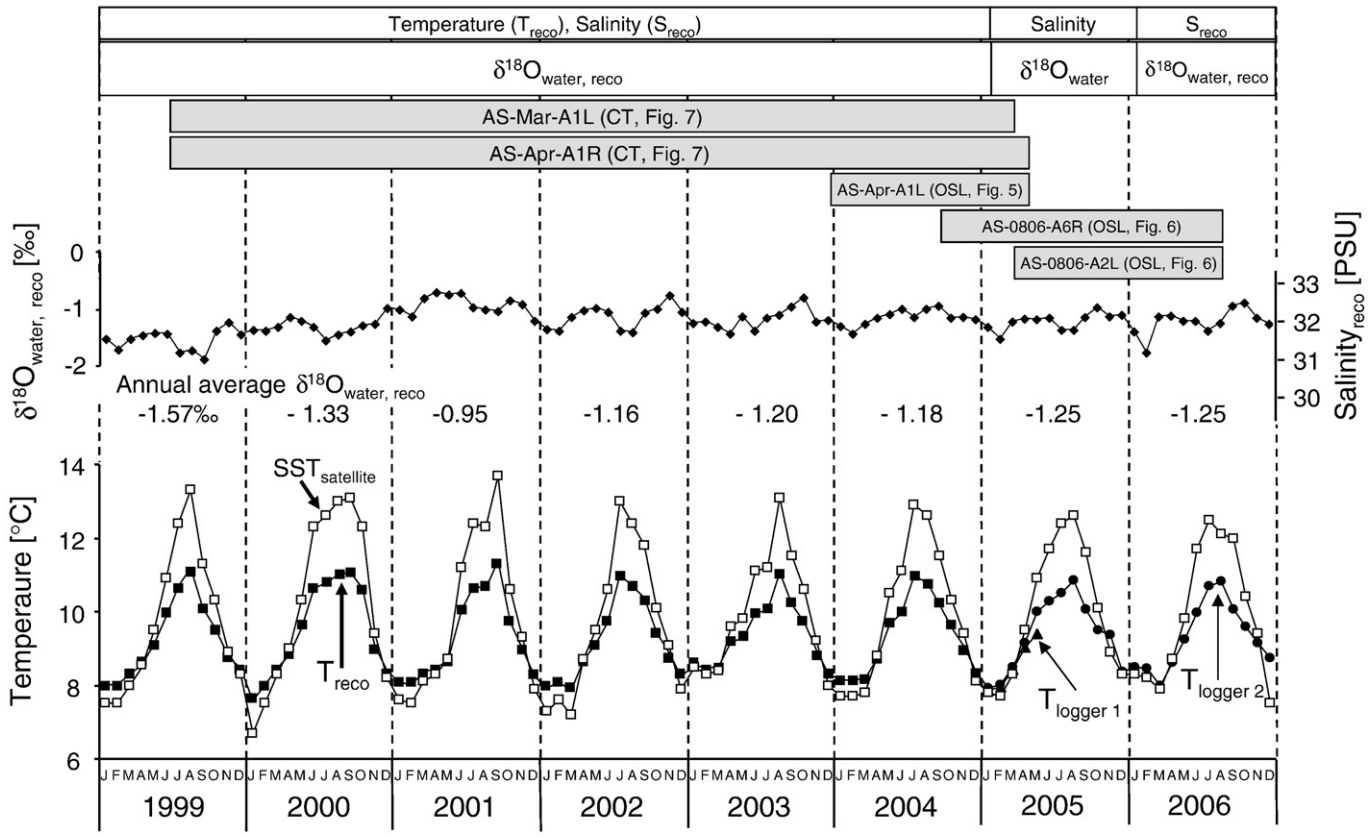

Fig. 4. Hourly resolved temperature data (T_{logger}, 2005–2006; logger 1: triangles, logger 2: filled circles) and bi-weekly to monthly water samples ($\delta^{18}O_{water}$+salinity, 2005) were obtained from the position where the shells lived. For other time intervals from 1999–2006, monthly resolved environmental records were reconstructed (T_{reco}: filled squares; S_{reco}+$\delta^{18}O_{water, reco}$: filled diamonds) from satellite data (open squares), published data and meteorological stations nearby (for details see text). The temporal coverage of the shell oxygen isotope records of the outer shell layer (OSL) and cardinal tooth (CT) records is indicated by the grey bars.

during growth (Epstein et al., 1953). The shell mineralogy of *P. abrupta* is the $CaCO_3$ polymorph aragonite (Coan et al., 2000). This was confirmed by the present study. According to Raman analyses the outer and inner shell layers equally consist of more than 95% aragonite. Thus, we utilized the paleothermometry equation by Böhm et al. (2000) for biogenic aragonite to reconstruct temperatures from $\delta^{18}O_{shell}$ values:

$$T_{\delta^{18}O}(°C) = (20 \pm 0.2) - (4.42 \pm 0.1) \cdot \left(\delta^{18}O_{shell} - \delta^{18}O_{water}\right) \quad (1)$$

A one per mil shift in the $\delta^{18}O_{shell}$ value corresponds to a temperature change of the ambient water by 4.42 °C. The equation by Böhm et al. (2000) is superior to the Grossman and Ku (1986) function because it provides more reliable data and reduces the error. If the $\delta^{18}O_{shell}$ and $\delta^{18}O_{water}$ values are the same, the temperature error equals ±0.2 °C. With each one per mil increase in the difference between the two values, the temperature error increases by ±0.1 °C. For temperature error estimates, the precision error of the mass spectrometer was also considered. In the present study, the average error was ±0.5 °C.

2.5. Environmental recordings

In order to calibrate shell growth and the $\delta^{18}O_{shell}$ data, we recorded temperature, salinity and the oxygen isotope composition ($\delta^{18}O_{water}$) at the locality where the shells lived (Figs. 4 and 6, Table 2). Two temperature loggers (HOBO Water Temp Pro v2) were deployed near Protection Island at water depths of 11 and 14 m, respectively. The first logger (11 m) recorded bottom water temperatures on an hourly basis from 27 January to 3 May 2005 before it was lost. The second temperature logger was deployed approximately 0.9 km north of the first logger at N48°07.253, W122°57.156 (14 m) and provided seawater temperature data at hourly intervals for almost 2 yr (27 January 2005 to 4 December 2006) (Figs. 4 and 6). An arithmetic average, T_{logger}, was calculated from the two loggers and used for the comparison with the shell data (Fig. 6). Aside from a seasonal oscillation, T_{logger} data fluctuated on a fortnightly time-scale. During spring tides, temperatures were higher than during neap tides (Fig. 6). Daily temperature ranges were as large as 2.3 °C during summer, but negligibly small (0.1 °C) during winter (Fig. 6). The minimum and maximum recorded temperatures were 7.8 °C (6 February 2005, 3:00 PM) and 12.3 °C (8 July 2006, 7:00 AM), respectively. The average T_{logger} equaled ca. 9.5 °C in 2005 (Table 3). The precision of the logger data was ±0.2 °C. Because no bottom water temperature data were available for Protection Island for the time interval of January 1999 to January 2005, we used monthly resolved satellite data, $SST_{satellite}$ (AVHRR Pathfinder SST v5 Product 216; Physical Oceanography DAAC at podaac-www.jpl.nasa.gov), to reconstruct these values for Protection Island (T_{reco}) (Figs. 1, 2, 4–7). $SST_{satellite}$ and T_{logger} data were linearly correlated (R=0.98, R^2=0.96, p<0.0001). Based on the linear regression analysis, T_{reco} can be inferred from $SST_{satellite}$ with the following equation:

$$T_{reco} = \frac{SST_{satellite} + 7.21}{1.83}. \quad (2)$$

For $\delta^{18}O_{water}$ analyses, SCUBA divers collected water samples in close vicinity to the shells on a bi-weekly to monthly basis from January 2005 to January 2006 (Table 2; Fig. 4). Bottles were rinsed

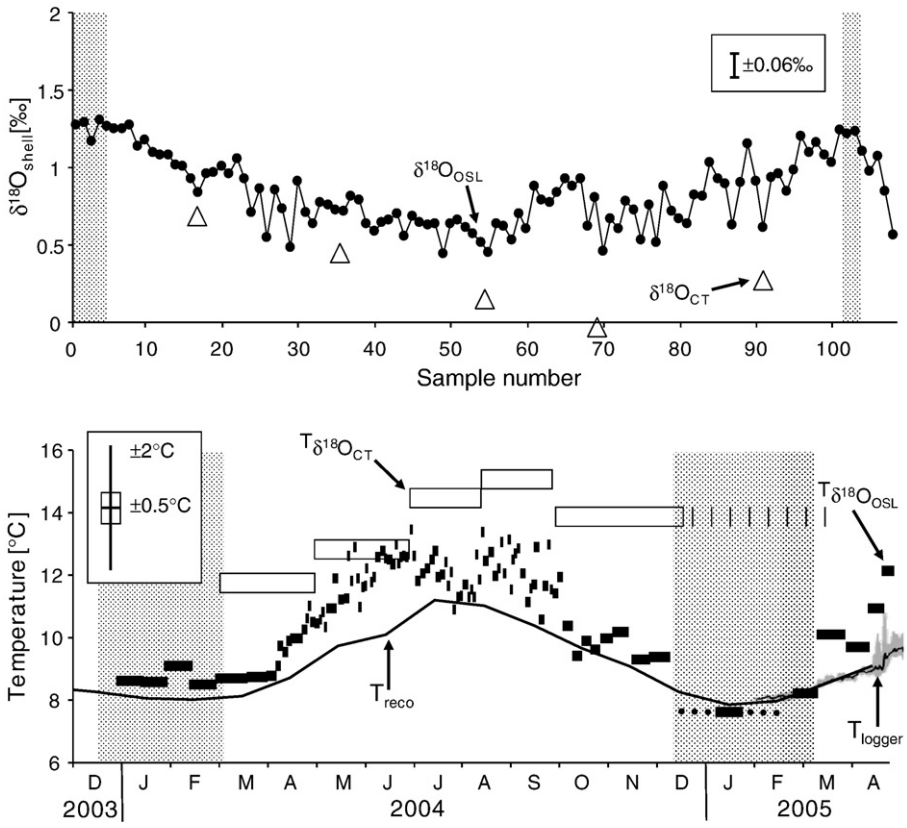

Fig. 5. Specimen AS-Apr-A1L: Shell oxygen isotope record (upper panel) and temperatures reconstructed thereof (lower panel). Black circles and black squares are data from the outer shell layer (OSL) near the ventral margin, open triangles and open squares represent data from the cardinal tooth (CT). The temporal coverage of each sample is indicated by the length of the bars (lower panel). Whether the shells grew during winter at extremely low rates or entirely ceased growing is difficult to tell (stippled or dotted lines). Shaded portions represent samples taken from the within annual growth lines. T_{reco} = monthly temperatures reconstructed from satellite data, T_{logger} = hourly resolved data (grey) and daily averages (black) from temperature loggers recorded from 27 January 2005 onwards. Error bar in the upper panel refers to the precision error of the mass spectrometer. Error bars in the lower panel represent the average errors of all $T_{\delta 18O}$ data of this study. The 0.5 °C error is computed from the Böhm et al. (2000) paleotemperature equation including the precision error of the mass spectrometer. The 2 °C error considers the seasonal salinity and oxygen isotopy of the water ($\delta^{18}O_{water}$ or $\delta^{18}O_{water,\ reco}$) variability. $T_{\delta 18O}$ calculation is based on annual average $\delta^{18}O_{water}$ or $\delta^{18}O_{water,\ reco}$. In general, T_{reco} are fairly well reproduced by $T\delta^{18}O_{OSL}$, but overestimated by $T\delta^{18}O_{CT}$. Note the different temporal resolution of the data sets. T_{reco} is monthly resolved, each $T\delta^{18}O_{OSL}$ represents up to 2 days, and $T\delta^{18}O_{CT}$ approx 1.5 to 2 months per sample. Note, that the daily temperatures during summer exhibit a range of up to 2.3 °C (see Fig. 6, lower panel).

several times and the lid was tightly closed. Samples were refrigerated at 4 °C prior to the analyses. 7 ml of water was equilibrated in 13 ml headspace with gaseous CO_2 in an automated equilibration device connected to a Finnigan MAT Delta-S mass spectrometer. The $\delta^{18}O_{water}$ values are reported against VSMOW (Vienna Standard Mean Ocean Water). Average 1SD error was better than 0.03‰. Slight variations in $\delta^{18}O_{water}$ can significantly alter temperature estimates from shell oxygen isotopes. For example, a change in $\delta^{18}O_{water}$ of 0.1‰ results in a temperature difference of more than 0.4 °C. Because $\delta^{18}O_{water}$ values fluctuated with the tides, annual $\delta^{18}O_{water}$ averages were computed in order to reconstruct water temperatures from $\delta^{18}O_{shell}$ values. Seasonal minimum and maximum $\delta^{18}O_{water}$ values were used for an additional error calculation of the shell oxygen isotope-derived temperatures (here, on average, ±2 °C). Salinity of the water samples was measured to the nearest of 1 PSU. The $\delta^{18}O_{water}$ values varied between −1.44‰ and −1.05‰ (Table 2) with an average value of −1.27‰ during 2005, and salinity ranged from 31 to 32 PSU (2005 average: 31.9 PSU).

Oxygen isotope values of the water for the time interval of January 1999 to December 2006 were reconstructed ($\delta^{18}O_{water,\ reco}$) from monthly salinity (S) records of a lighthouse, Race Rocks (W 123° 31.548, N 48° 17.541), ca. 50 km northwest of Protection Island (Fig. 1). We used a linear regression model of salinity and $\delta^{18}O_{water}$ of the Northwest Pacific (Fig. 1, N44–54°, W126–158°). These data (Epstein and Mayeda, 1953; Craig and Gordon, 1965) were obtained from NASA Goddard Institute for Space Studies from their homepage at http://data.giss.nasa.gov/o18data/:

$$\delta^{18}O_{water,reco} = 0.67*S - 22.8 \quad (R = 0.81; R^2 = 0.66, p = 0.004, n = 10). \tag{3}$$

Measured and reconstructed oxygen isotope values of the water during 2005 showed a constant offset of ca. 0.7‰ indicating that seawater at Race Rocks was about 1 PSU fresher than at Protection Island. Therefore, we added 1 PSU to each Race Rock salinity value und used these data to calculate the $\delta^{18}O_{water,\ reco}$ for Protection Island. During 1999–2006, the $\delta^{18}O_{water,\ reco}$ ranged from −1.92‰ to −0.75‰, while salinity values were between ca. 31.06 PSU and 32.82 PSU (Fig. 4). A seasonal cycle does not exist. However, from 1999 to 2001, waters became more saline (seasonal averages; 31.5 to 32.5 PSU), thereafter a shift toward slightly fresher conditions was observed (32 PSU). $\delta^{18}O_{water,\ reco}$ values of 2005 (−1.25‰) were in perfect agreement with the average $\delta^{18}O_{water}$ value of −1.27‰.

3. Results

Specimens immersed in Mutvei's solution permitted an easy identification of shell internal growth patterns (Fig. 3). In cardinal tooth sections, sharply delimited annual growth lines separated consecutive annual growth increments from each other (Fig. 3A). In

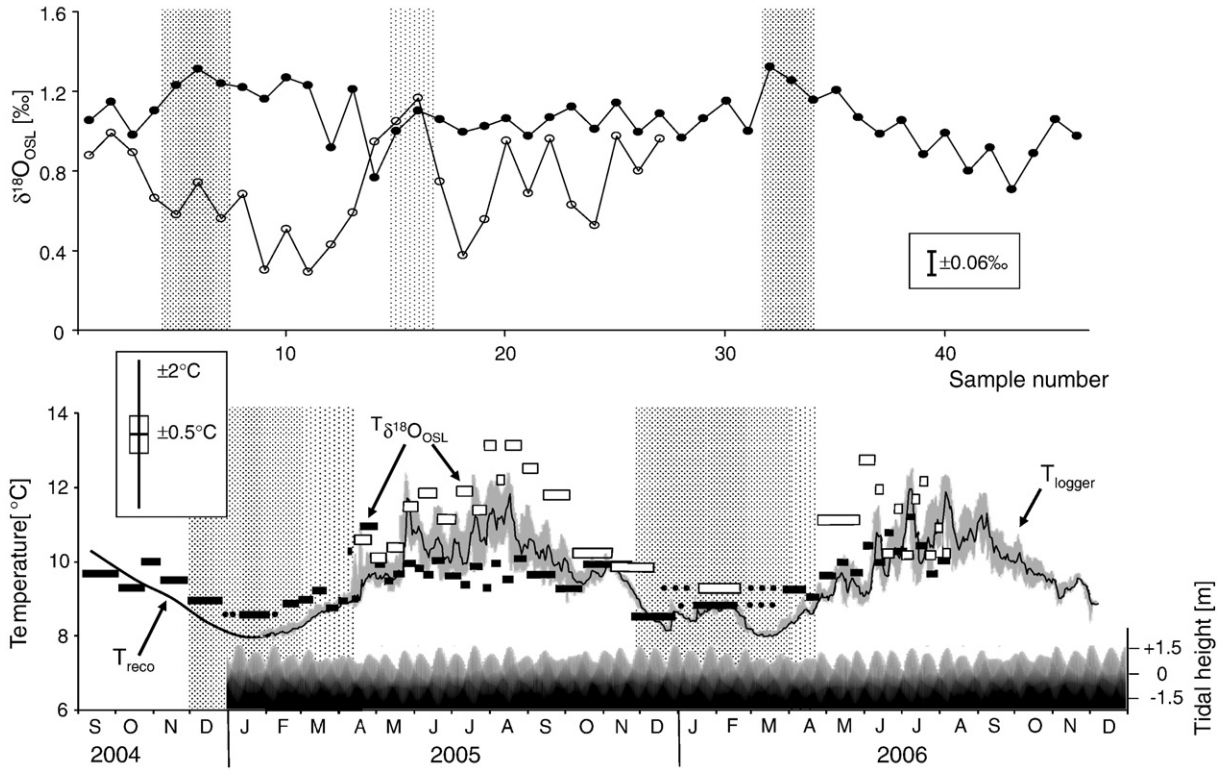

Fig. 6. Specimens AS-0806-A2L (filled circles and squares) and AS-0806-A6R (open circles and squares): Shell oxygen isotope records from the outer shell layers (upper panel) and temperatures reconstructed thereof (lower panel). Despite both shells occurred contemporaneously at the exact same locality, their isotope records and $T\delta^{18}O_{OSL}$ data differ greatly from each other. The temperature record of specimen AS-0806-A2L appears truncated, whereas specimen AS-0806-A6R overestimates the temperature logger data, particularly during summer. Dark shading represents position of annual growth lines in specimen AS-0806-A2L, light shading that of specimen AS-0806-A6R. Note that daily summer temperatures exhibit a range of up to 2.3 °C (grey curve in lower panel; average daily T_{logger} data in black). This variability is strongly related to the tides. For other details of the graphs see description in caption of Fig. 5.

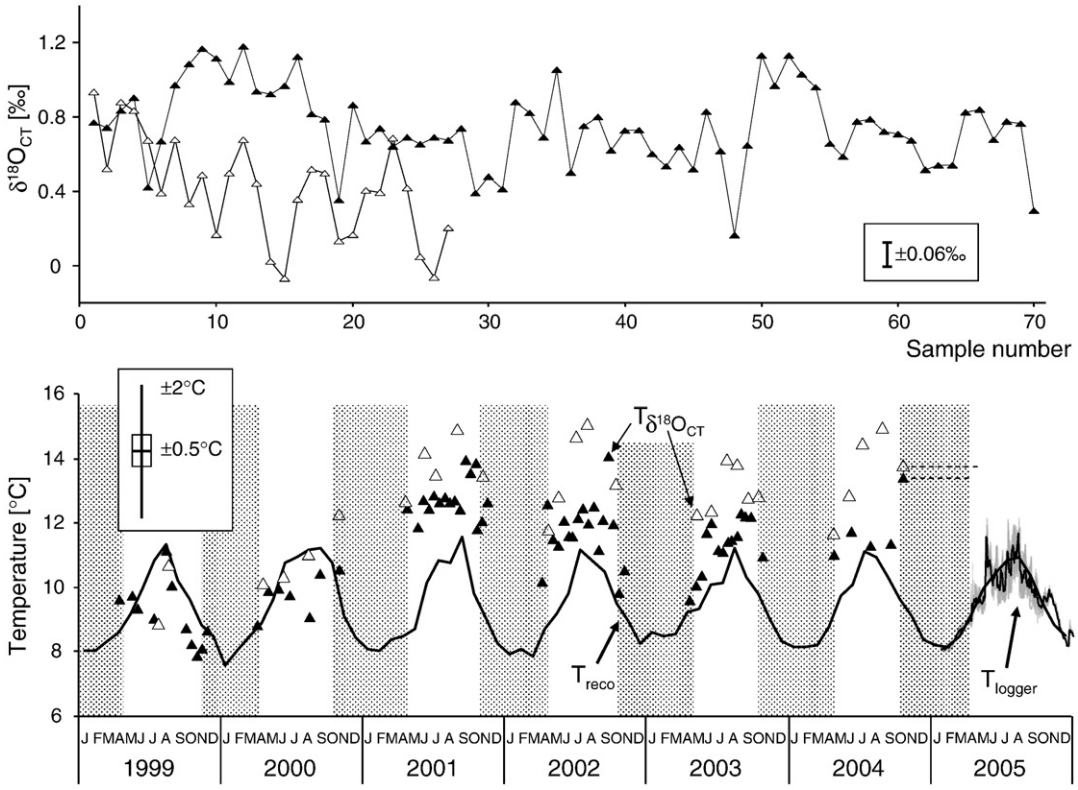

Fig. 7. Specimens AS-Mar-A1L (filled triangles) and AS-Apr-A1L (open triangles): Shell oxygen isotope records from the cardinal teeth (CT) (upper panel) and temperatures reconstructed thereof (lower panel). Actual temperatures were greatly overestimated by the shell record during 2001 to 2004, particularly from specimen AS-Apr-A1L. Note that this specimen exhibited a distinct trend toward less positive $\delta^{18}O_{CT}$ values with increasing age. For other details of the graphs see description in caption of Fig. 5.

Table 2
List of water samples used in the present study

Date of collection	Locality	Water depth	$\delta^{18}O_{water}$	S	S_{reco}
		(m)	(‰)	(PSU)	(PSU)
27 January 2005	N48°07.794, W122°57.400	11	−1.37±0.012	32	31.98
2 February 2005	N48°08.753, W122°57.156	14	−1.30±0.01	31	31.88
9 February 2005	N48°08.278, W122°57.164	15	−1.44±0.025	32	31.78
23 February 2005	N48°08.198, W122°57.194	14	−1.27±0.014	32	32.04
24 March 2005	N48°08.253, W122°57.156	13	−1.09±0.029	32	32.31
7 April 2005	N48°08.768, W122°57.091	12	−1.28±0.009	32	32.02
15 June 2005	N48°08.253, W122°57.156	13	−1.19±0.002	32	32.15
2 August 2005	N48°07.794, W122°57.400	11	−1.41±0.014	32	31.83
8 December 2005	N48°08.253, W122°57.156	15	−1.05±0.009	32	32.37
11 January 2006	N48°08.253, W122°57.156	15	−1.36±0.012	32	31.90

Salinity (S) was measured to the nearest 1 PSU. The freshwater mixing line enabled a calculation of salinity (S_{reco}) values from isotope values of the water ($\delta^{18}O_{water}$).

the outer shell layer, however, these annual growth structures were much more difficult to track, because the growth lines approached the outer shell surface at a very narrow angle (approx. 10°; Fig. 3B). During the first 10–15 yr of life, *Panopea abrupta* shells grew predominantly in shell size and formed the broadest annual increments (up to 956 µm in the cardinal tooth). Subsequently, the shells grew mainly in ventral margin thickness (= "inward growth", Zolotarev, 1980). After the age of fifteen, increment widths in the cardinal tooth measured only between 8 and 172 µm. The ventral margin thicknesses ranged from 0.6 mm in a six year-old shell (AS-Apr-A1L) to 2.23 mm in a 63 year-old specimen (AS-0806-A4L) (Table 1).

The first few centimeters of the shells (measured along the outer shell surface and along shell height) were dominated by the inner shell layer (Fig. 2B). Only at approximately 2 cm from the umbo could the outer shell layer be identified. The inner shell layer vanished at ca. 7 cm from the umbo while the outer shell layer continued to increase in thickness toward the ventral margin (Fig. 2B). It should be noted that the cardinal tooth only yielded a minimum estimate of the ontogenetic age of the bivalve. According to a comparison of relative annual increment widths of the outer shell layer and the cardinal tooth, the first ca. 3 yr of life may be missing in the cardinal tooth due to dissolution.

3.1. Shell oxygen isotope data

A total of 278 oxygen isotope samples of four different shells ($\delta^{18}O_{shell}$) were analyzed (Table 1; Fig. 4). 181 samples came from the outer shell layer near the ventral margin ($\delta^{18}O_{OSL}$) of three specimens, namely AS-Apr-A1 (n=108; Fig. 5), AS-0806-A2L (n=27; Fig. 6), and AS-0806-A6R (n=46; Fig. 6). The $\delta^{18}O_{OSL}$ values exhibited very high temporal resolution of up to two days per sample as they only covered the years of 2004–2006. The remaining 97 samples were taken from the cardinal tooth sections ($\delta^{18}O_{CT}$; inner shell layer) of specimens AS-Mar-A1L (n=70; Fig. 7) and AS-Apr-A1 (n=27; Fig. 7), respectively, representing mainly the time interval of 1999 to 2004 (little shell material had formed between winter 2004/2005 and the date of collection in spring 2005).

Table 3
Temperature data

2005	T_{logger}		
	(°C)		
	Monthly resolution	Daily resolution	Hourly resolution
Average	9.37	9.49	9.49
Minimum	7.93	7.91	7.77
Maximum	10.84	11.72	12.22
Amplitude	2.91	3.81	4.45
2004	T_{reco}		
	(°C)		
	Monthly resolution		
Average	9.31		
Minimum	10.97		
Maximum	8.13		
Amplitude	2.84		

Seasonal amplitudes, average and extreme temperatures from logger data (T_{logger}) during 2005 and satellite-based reconstructed temperatures (T_{reco}) during 2004.

3.2. Differences between $\delta^{18}O$ records of the inner and outer shell layer

Distinct seasonal oscillations were observed in all oxygen isotope chronologies from the outer shell layer with most positive values near the annual growth lines and least positive values half-way between two consecutive annual growth lines (Figs. 5 and 6). However, the $\delta^{18}O_{CT}$ curves showed less clear sinusoidal oscillations, particularly specimen AS-Mar-A1 (Fig. 7). In addition, the $\delta^{18}O_{CT}$ curve of specimen AS-Apr-A1 exhibited a distinct trend from an annual average of 0.73‰ in 1999 to 0.26‰ in 2004 (Fig. 7). Specimen AS-Mar-A1, however, showed a much weaker trend from 0.88‰ to 0.67‰ during the same time interval (Fig. 7). A direct comparison of the $\delta^{18}O_{CT}$ and $\delta^{18}O_{OSL}$ data was possible for specimen AS-Apr-A1 (Fig. 5). On average, $\delta^{18}O_{CT}$ values of 2004 of this specimen were 0.58‰ more negative than the $\delta^{18}O_{OSL}$ data. Extreme $\delta^{18}O_{CT}$ values equaled −0.06 and 0.69‰ (n=5; Table 4), whereas those of the outer shell layer were 0.44 and 1.31‰ (n=102). Seasonal amplitudes recorded in the cardinal tooth (0.75‰) compared well to those of the outer shell layer record (0.87‰) (Table 4). Note that these differences occurred despite much lower sampling resolution in cardinal tooth sections than in the outer shell layer (five versus 102 samples).

3.3. Variability of $\delta^{18}O$ records among different contemporaneous specimens

Notably, the $\delta^{18}O$ values of contemporaneous shells from the same habitat differed significantly from each other (Figs. 6 and 7). As mentioned above, the $\delta^{18}O_{OSL}$ data showed differences of up to 0.40‰ among individuals AS-0806-A2 and AS-0806-A6 (Fig. 6). Although both specimens grew contemporaneously at the same locality their oxygen isotope profiles varied in respect to amplitude and absolute values (Fig. 6, Table 4). The average value of 2005 calculated from

Table 4
Shell (*Panopea abrupta*) oxygen isotope-derived temperatures

Shell portion	Time interval ($\delta^{18}O_{water,reco}$ or $\delta^{18}O_{water}$ [‰])		$\delta^{18}O_{shell}$ [‰] ($T_{\delta 18O}$ [°C])			
			AS-Mar-A1	AS-Apr-A1	AS-0806-A2	AS-0806-A6
OSL	2004 (−1.18)	Average		0.84 (11.1)		
		Maximum		1.31 (9)		
		Minimum		0.44 (12.8)		
		Amplitude		0.87 (3.8)		
	2005 (−1.27)	Average			0.7 (11.3)	1.1 (9.5)
		Maximum			1.17 (9.2)	1.32 (8.6)
		Minimum			0.29 (13.1)	0.76 (11)
		Amplitude			0.88 (3.9)	0.56 (2.4)
CT	2004 (−1.18)	Average	0.67 (11.8)	0.26 (13.6)		
		Maximum	0.84 (11.1)	0.69 (11.8)		
		Minimum	0.30 (13.5)	−0.06 (15.1)		
		Amplitude	0.54 (2.4)	0.75 (3.3)		
	1999–2004 (see Fig. 4)	Average	0.75 (11.4)	0.42 (12.9)		
		Maximum	1.18 (7.9)	0.94 (8.9)		
		Minimum	0.16 (14.2)	−0.07 (15.1)		
		Amplitude	1.02 (6.3)	1.00 (6.2)		

Seasonal amplitudes, average and extreme oxygen isotope values ($\delta^{18}O_{shell}$) and temperatures reconstructed thereof ($T_{\delta 18O}$). OSL = outer shell layer, CT = cardinal tooth.

specimen AS-0806-A6 (1.10‰; $n=28$) was 0.40‰ more positive than that of AS-0806-A2 (0.70‰, $n=16$; Table 4). During 2005, minimum and maximum $\delta^{18}O_{OSL}$ values of specimen AS-0806-A6 were 0.76 and 1.32‰ (amplitude of 0.56‰), whereas specimen AS-0806-A2 exhibited extremes of 0.29 and 1.17‰ (amplitude of 0.88‰). Notably, the isotope record obtained from AS-0806-A6 was ca. 80% higher resolved than that of its neighbor. Likewise, the cardinal tooth records differed from each other. The record of specimen AS-Apr-A1 showed a distinct trend over the time interval of 1999–2004 (Fig. 7). Consequently, the average $\delta^{18}O_{CT}$ values of the shells AS-Mar-A1 (0.75‰; $n=70$) and AS-Apr-A1 (0.42‰; $n=27$) differed by 0.33‰ (Table 4).

3.4. Timing of shell growth

In order to assign precise calendar dates to each portion of the shells, expected $\delta^{18}O$ values ($\delta^{18}O_{exp}$) were computed from instrumental or modeled temperatures (T_{logger}, T_{reco}) and oxygen isotope values of the water ($\delta^{18}O_{water}$, $\delta^{18}O_{water,\ reco}$) values using the equation by Böhm et al. (2000). The $\delta^{18}O_{shell}$ values from the very tip of the shells (= date of collection) functioned as one important anchor point. Then, shell oxygen isotope data of the shells were so arranged that measured and expected oxygen isotope curves closely matched each other, and the best fit was obtained between the $\delta^{18}O_{exp}$ and $\delta^{18}O_{shell}$ data (qualitative wiggle matching, linear regression analyses). Correlation coefficients were as high as $R=0.82$ ($p<0.0001$; AS-Apr-A1, OSL). After the temporal alignment of the data was completed, temperatures were calculated from shell oxygen isotope data and plotted against time (Figs. 5–7).

3.5. Temperature reconstructions from shell oxygen isotopes

As seen from Figs. 5 and 6, shell growth of the outer shell layer (OSL) mainly occurred between March/April and November/December. Lowest $T_{\delta 18O}$ fell together with the annual growth lines. The agreement between temperatures derived from shell oxygen isotopes of the OSL ($T\delta^{18}O_{OSL}$) and instrumental or modeled temperatures varied from shell to shell.

The $T\delta^{18}O_{OSL}$ of the youngest sampled specimen (AS-Apr-A1, 6 yr old) showed the closest match with T_{reco} (Fig. 5). $T\delta^{18}O_{OSL}$ overestimated actual minimum (8.1 °C) and maximum (11 °C) temperatures during 2004 by 0.9 °C and 1.8 °C, respectively, and the seasonal range (2.8 °C) by 1 °C (Tables 3 and 4). Note the different time averaging of both data sets: T_{reco} are monthly values, whereas the temporal resolution of the $T\delta^{18}O_{OSL}$ of this specimen was ca. two days during summer and about one to two weeks during winter. T_{logger} data from 2005 suggested a large daily temperature range during summer of more than 2.3 °C and 1 °C larger seasonal amplitude than that calculated from monthly values (Table 3; Fig. 6). Although the reconstructed summer temperatures of AS-Apr-A1 tended to slightly overestimate the actual values, winter temperatures were almost perfectly reproduced. Notably, the error bars of the $T\delta^{18}O_{OSL}$ encompass the observed monthly temperatures.

The $T\delta^{18}O_{OSL}$ records of the other two shells that lived contemporaneously at the same locality differed significantly from one another in range, average and summer values (Fig. 6). Specimen AS-0806-A6 (16 yr old) showed a truncated seasonal temperature amplitude barely exceeding 2.4 °C (winter and summer extremes of 8.6 °C and 11 °C; Table 4). Despite that, the upper error bars of the reconstructed temperatures of this shell were still in the bounds of measured temperatures (Fig. 6). However, the $T\delta^{18}O_{OSL}$ curve of the 25 year-old specimen AS-0806-A2 was shifted toward warmer temperatures by an average of 2 °C during summer with the error bars plotting outside the daily temperature variance (Fig. 6). The reconstructed seasonal temperature range of 3.9 °C was in good agreement with daily T_{logger} data, but both daily winter (7.9 °C) and summer (11.7 °C) extremes were overestimated by the shell isotope record (about two weeks resolution) by ca. 1.4 °C (Tables 3 and 4). The annual average $T\delta^{18}O_{OSL}$ of the two shells differed by 1.8 °C.

Temporally aligned temperature estimates from cardinal teeth ($T\delta^{18}O_{CT}$) differed greatly from each other (up to 4 °C) and exceeded actual temperatures by more than 3–4 °C in some years (Fig. 7). Seasonal temperature extremes showed less severe discrepancies (Table 4). For example, summer $T\delta^{18}O_{CT}$ maxima during 2004 were 13.5 °C and 15.1 °C in the six year-old specimens AS-Mar-A1 and AS-Apr-A1, respectively. Note that each sample from AS-Apr-A1 represented more than one month, whereas a ca. bi-weekly resolution was achieved for specimen AS-Mar-A1. Lowest $T\delta^{18}O_{CT}$ values (2004) of specimen AS-Apr-A1 equaled 11.8 °C which is ca. 2.5 °C warmer than observed during winter. Its $T\delta^{18}O_{CT}$ range (3.3 °C), however, was almost identical to the observed seasonal amplitude (monthly resolution).

It was difficult to confidently add a time axis the $T\delta^{18}O_{CT}$ data, particularly in the case of specimen AS-Mar-A1. The record may be incomplete and did not display seasonal oscillations. Over the time interval of 2001–2004, however, both reconstructed temperature curves plotted above the T_{reco}, while actual temperatures were underestimated during 1999.

3.6. Intra-annual shell growth rates and relation to temperature

Based on the temporal alignment of the $\delta^{18}O_{OSL}$ data it was possible to estimate the time represented by each isotope sample. In turn, this enabled us to estimate the relative monthly growth rates during different seasons (Fig. 8). Growth rate increased rapidly after the winter cessation and reached a maximum in late spring and summer. After August shell growth quickly slowed down and reached minimum rates in November or December. Shell growth and temperature were highly positively correlated. For example, reconstructed monthly shell growth of the 25 year-old specimen AS-0806-A2 showed a strong positive linear correlation with water temperature ($R=0.93$, $R^2=0.86$, $p<0.0001$).

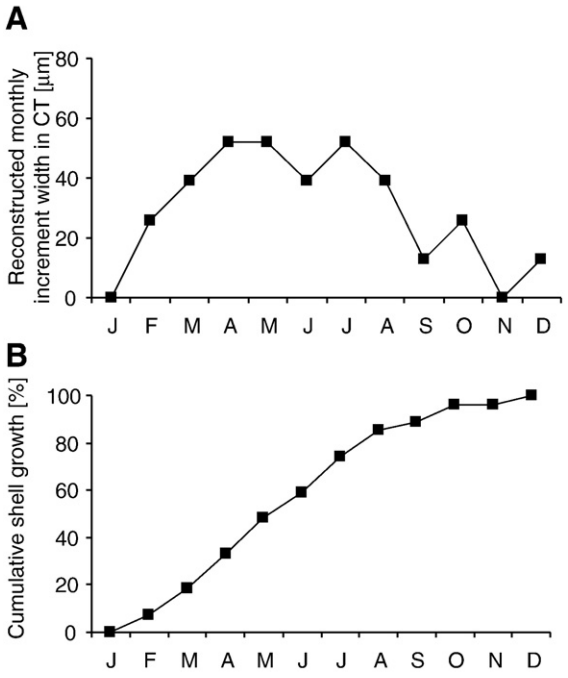

Fig. 8. Relative monthly shell growth rates (A = differential; B = integral, cumulative growth curve) during different seasons. Growth rate increased rapidly after the winter cessation and reached a maximum in late spring and summer. After August shell growth quickly slowed down and reached minimum rates in November or December (specimen AS-0806-A2L).

4. Discussion

Owing to its remarkably long lifespan, *Panopea abrupta* has recently become the focus of paleoclimate reconstructions (Strom et al., 2004, 2005). These studies have demonstrated that shell growth of this species is influenced by the PDO (Strom et al., 2004). However, little is known about intra-annual growth rates and whether geochemical proportions of geoducks can be used to quantitatively reconstruct past water temperatures and other environmental variables (compare Goman et al., 2007). The present study is the first to compare the high-resolution (up to two days per sample) oxygen isotope records of contemporaneous shells from the same habitat with each other and with high-resolution environmental data, including hourly resolved instrumental temperatures and near-monthly $\delta^{18}O_{water}$ records. Results of our study suggest that shell oxygen isotopes of this species may be more challenging to interpret than previously thought (Goman et al., 2007). For example, the study by Goman et al. (2007) did not take into account that $\delta^{18}O_{water}$ values can change significantly on seasonal and inter-annual time-scales. The authors reported only a single $\delta^{18}O_{water}$ measurement. Furthermore, their study was only based on two specimens and did not address possible inter-individual differences of $\delta^{18}O_{shell}$ values. In addition, analyses were only performed on the hinge plate, a shell portion that should not be used for chemical analyses.

4.1. Timing of shell growth

Temporally aligned shell oxygen isotope profiles indicated that the main growing season (= formation of the annual growth increment) of *P. abrupta* lasts from March or April through November or December (Figs. 5 and 6). During the remainder of the year, however, the annual growth line seems to form. These findings compare well with the work by Shaul and Goodwin (1982). In fact, geoducks are less active in winter and have their siphons retracted most of the time (Goodwin, 1977) so that shell growth is reduced to extremely low rates (Shaul and Goodwin, 1982). Slight variations in the duration of the growing season may be explained by year-to-year environmental variability (temperature, food etc.) or different individual physiological needs. However, there is no trend toward shorter growing periods with increasing ontogenetic age as in some short-lived bivalve species (e.g., Miyaji et al., 2007). Knowledge of the timing of shell growth and its possible changes throughout life is relevant to interpret long-term climate data gathered from biogenic hard parts (Schöne et al., 2005c). Former studies have provided indirect evidence for a temporally invariable growing period of geoduck shells. Strom et al. (2004, 2005) showed that annual increment chronologies from contemporaneous specimens of different ontogenetic ages matched each other perfectly. If the duration of the growing season was reduced with increasing age, the corresponding annual increments would be narrower and the growth curves of these individuals would not have compared well with each other.

4.2. Oxygen isotope variability among shells

Oxygen isotope-derived temperature records of the OSL of contemporaneous shells from the exact same habitat varied by up to 2 °C from each other (Fig. 6). This can barely be explained by microhabitat differences, because the surface waters were well-mixed at the locality where the shells dwelled. Near Protection Island, temperature and salinity values are unlikely to vary on scales of nearly 2 °C (=50% of the seasonal temperature amplitude; compare Fig. 4) or 0.7 PSU (=140% of the seasonal salinity amplitude; compare Fig. 4) within a few meters. Furthermore, differences in sample resolution cannot account for the observed differences in $\delta^{18}O_{OSL}$ values. Yet, the lowest number of samples came from specimen AS-0806-A2 (Fig. 6), this shell was isotopically most depleted. Vital effects (Urey et al., 1951; Weiner and Dove, 2003) can also be ruled out, because shell calcium carbonate utilizes the oxygen isotopes of the water and not oxygen of the food. A more likely explanation for the discrepancies is that variable exchange rates between the outer EPF (extrapallial fluid) and the ambient water vary among different specimens. During $CaCO_3$ precipitation, the EPF becomes isotopically depleted, because ^{18}O is preferably incorporated into the shell. This has been demonstrated by numerous experimental (e.g., Epstein et al., 1953; Grossman and Ku, 1986) and theoretical studies (O'Neil et al., 1969). The $\delta^{18}O_{OSL}$ values of newly forming shell will therefore be more negative. The observed greater discrepancy between expected and measured shell oxygen isotope values can be explained by higher growth rates in summer which will cause a stronger depletion in ^{18}O of the EPF. Although bivalves are generally believed to precipitate their hard parts (at least the outer shell layer) in isotopic equilibrium with the ambient water, slight between-specimen differences have been also reported in various other studies (Goodwin et al., 2001; Schöne et al., 2006; Gillikin et al., 2005).

In addition, we observed some variability in the seasonal temperature amplitudes of up to 1.5 °C (Figs. 5 and 6, Tables 3 and 4). The $T\delta^{18}O_{OSL}$ curve of specimen AS-0806-A6 appeared flatter than that of specimen AS-0806-A2 (Fig. 6). The latter overestimated summer temperatures more than winter temperatures (Tables 3 and 4). It is possible that the specimens deposited shell at different times during the day. Analyses of physiological activity patterns of bivalves held in tanks revealed considerable variability in the timing of shell gaping between different species (Rodland et al., 2006), but also among different individuals of the same species (unpublished data by one of us, BRS). No specimen grew uninterruptedly during the day, but showed clear circadian and ultradian activity cycles. For example, *Anodonta cygnea* (Linnaeus) is physiologically active and precipitates shell carbonate only during ca. 8–12 h per day. In settings with intra-annual temperature variations, the timing of shell formation during one day/night cycle can result in very different shell oxygen isotope curves. In this study, temperature loggers indicated an intra-daily temperature variability of up to 2.3 °C during summer (Fig. 6), which corresponds to more than 50% of the seasonal temperature amplitude. If one geoduck, for example, grew preferentially during midday, the resulting $T\delta^{18}O_{OSL}$ curve would exhibit a greater seasonal amplitude (see AS-0806-A6; Fig. 6) than the temperature record of a specimen that grew preferentially at night (see AS-0806-A2; Fig. 6).

It remains unclear what caused these individual differences in ultradian timing of shell growth. Variable ultradian activity patterns could be linked to genetically predetermined or environmentally entrained physiological differences. The underestimation of summer temperatures by the $T\delta^{18}O_{OSL}$ values of specimen AS-0806-A6 may also be explained by siphon-cropping. According to Nakaoka (2000) the presence of predators can alter the feeding behavior of bivalves. Siphon-cropping by epibenthic vertebrates and invertebrates like crabs, sea stars and gastropods may not directly result in death, but can have negative, sublethal effects on bivalve growth and feeding. While more energy is spent on tissue regeneration, the feeding rate is reduced and thus shell growth rates are lower (Peterson and Quammen, 1982). Foraging predators may be particularly abundant and active during the warm season of the year. Subtidal predation of geoducks by epibenthic predators such as sea stars (*Pycnopodia* spp.) and Dungeness crabs (*Cancer magister* Dana) has been observed in the Puget Sound region (Lynn Goodwin, pers communication), and geoduck siphon tips have been recovered from the stomachs of cabezon and rockfish.

4.3. Oxygen isotope variability within shells

Cardinal teeth and the adjacent hinge plate of geoducks have previously been identified as the most suitable shell portions for growth pattern analyses (Shaul and Goodwin, 1982; Strom et al., 2004,

2005). However, our results suggest that the $\delta^{18}O_{shell}$ data from these shell portions should not be used for paleotemperature estimates. The $\delta^{18}O_{CT}$ ranges were shifted away from equilibrium and the $\delta^{18}O_{OSL}$ values by up to approx. 0.7–0.9‰ toward less positive values in most years (Fig. 7). This translates into a temperature overestimation of more than 3–4 °C and results in $T\delta^{18}O_{CT}$ values far outside the bounds of the instrumental temperatures and $T\delta^{18}O_{OSL}$. Note that the offset was also particularly high during our water sampling campaign and can hence not be explained by unrealistic estimates of the oxygen isotope values of the water. Whether this offset increases over a lifetime has yet to be shown. Moreover, the $\delta^{18}O_{CT}$ values of different contemporaneous specimens from the same habitat can also vary by nearly 4 °C (Fig. 7). One of the two sampled shells (AS-Apr-A1) showed a ca. 0.5‰ shift in its $\delta^{18}O_{CT}$ values while the oxygen isotope curve of the other specimen from the exact same locality showed only a minor negative shift of 0.2‰ during the same time interval (Fig. 7).

Although the cardinal tooth and outer shell layer consist of exact same mineralogy (>95% aragonite), the isotopic difference between the records of the two shell portions was not completely unexpected. The inner shell layer – which includes the cardinal tooth – and outer shell layer of many other bivalve mollusk species have been shown to vary considerably in respect to elemental composition and stable isotope ratios. For example, the outer prismatic and middle crossed-lamellar shell layers of *Mercenaria campechiensis* (Gmelin) differ greatly in respect to their Sr/Ca profiles (Surge and Walker, 2006). Likewise, the inner and outer shell layers of *Saxidomus giganteus* show a 0.2‰ difference in oxygen and carbon isotope data (Gillikin et al., 2005). It is well known that the cardinal tooth is precipitated from the inner EPF while the outer shell layer is formed from the outer EPF. These two fluids are probably not in elemental or isotopic equilibrium. Moreover, they may exhibit within- and among-specimen differences in the exchange rate between the EPF and the ambient water. Therefore geochemical analyses are commonly performed on shell material from the outer shell layer (Jones and Quitmyer, 1996).

4.4. Shell growth and water temperature

Seawater temperature is commonly the most important factor controlling shell growth in bivalves (Goodwin et al., 2001). For geoducks at Protection Island the fastest growth corresponded to the highest temperatures in July and August. During winter, however, growth was reduced or came to a complete cessation (Figs. 5, 6, 8). The relation between temperature and growth in geoduck shells was also postulated in previous studies (Noakes and Campbell, 1992; Strom et al., 2004) and demonstrated by laboratory experiments (Strom et al., 2004).

5. Conclusions

Paleoclimate reconstructions based on single geoduck shells appear to be highly problematic. Given a typical seasonal temperature range from about 8 to 12 °C, a nearly 2 °C discrepancy among the $T\delta^{18}O_{OSL}$ records of different specimens is a significant error and makes reliable paleotemperature estimates based on $\delta^{18}O_{shell}$ of *P. abrupta* nearly impossible. Another challenge encountered in this study was the need to interpret shell records that may have been biased towards higher or lower temperatures because the shells grew preferentially during night or day, or were exposed to high predation pressure. If additional shells from the same location and time-period were analyzed it may have been possible to provide a more robust estimate of the actual temperatures and to quantify the vital effects. Most paleoclimate analyses, however, are dependent on single specimens, because due to time-averaging contemporaneity of shells from the same stratigraphic horizon is almost impossible to prove.

Unknown paleo-$\delta^{18}O_{water}$ values further aggravate temperature estimates from $\delta^{18}O_{shell}$ values of this species. During a single year, $\delta^{18}O_{water}$ values can vary by ca. 0.39‰. This translates into a shell oxygen isotope-based temperature difference of 1.7 °C. Furthermore, ENSO and PDO strongly impact precipitation patterns in the Pacific Northwest (Walker, 1923; Kurtzman and Scanlon, 2007), freshwater discharge and hence the oxygen isotope composition of the water in which the shells live. Therefore, salinity and $\delta^{18}O_{water}$ values not only fluctuate on seasonal time-scales, but on decadal to multi-decadal time-scales as well.

Finally, although it may be more convenient to sample the same shell portion for isotope analyses that was used for growth pattern analysis, the cardinal teeth of geoducks exhibit strong vital effects in $\delta^{18}O_{shell}$ values. Temperature estimates from these inner layer shell portions may be incomplete and are usually precipitated out of equilibrium. This can result in a temperature overestimation by 3–4 °C and more.

Subsequent studies should analyze if the minor element to calcium ratios (Sr/Ca, Mg/Ca) of shells of *P. abrupta* can provide better paleotemperature estimates than stable oxygen isotope data. Perhaps, metal to calcium ratios can be used in conjunction with $\delta^{18}O_{shell}$ values to eliminate the adverse effect of variable $\delta^{18}O_{water}$ values on temperature reconstructions from oxygen isotopes.

Acknowledgments

We wish to acknowledge the late Tom O'Rourke for his critical contributions to the successful completion of this study. This work could not have been accomplished without the cooperation of the Jamestown S'Klallam Tribe and the efforts of their employees Tom, his wife Lohna O'Rourke and Aleta Erickson who together obtained all bottom samples of water and deployed and maintained the temperature loggers. We also thank Bob Lona, David Nguyen and the staff of the Washington Department of Health Biotoxin lab in Shoreline Seattle, who provided all shell samples. Analía Soldati is kindly acknowledged for her help with the Raman spectroscopy and A. Mackensen (Alfred Wegener Institute for Polar and Marine Research) for determining the $\delta^{18}O_{water}$ and salinity values. SST data (AVHRR) came from the PO.DAAC — NASA Jet Propulsion Laboratory from their Web site at http://www-sci.pac.dfo-mpo.gc.ca and salinity of Race Rocks from Fisheries and Oceans Canada — Pacific Region (http://www-sci.pac.dfo-mpo.gc.ca). Salinity and $\delta^{18}O_{water}$ values for the northwest Pacific were obtained from the NASA-Goddard Institute for Space Studies (http://data.giss.nasa.gov/o18data/). We thank two anonymous reviewers for their comments that helped further improving the manuscript. Financial support for this study was provided by the German Research Foundation, DFG (SCHO 793/3).

References

Böhm, F., Joachimski, M.M., Dullo, W.-C., Eisenhauer, A., Lehnert, H., Reitner, J., Wörheide, G., 2000. Oxygen isotope fractionation in marine aragonite of coralline sponges. Geochim. Cosmochim. Acta 64, 1695–1703.

Buick, D.P., Ivany, L.C., 2004. 100 years in the dark: extreme longevity of Eocene bivalves from Antarctica. Geology 32, 921–924.

Bureau, D., Hajas, W., Surry, N.W., Hand, C.M., Dovey, G., Campbell, A., 2002. Age, size structure and growth parameters of geoducks (*Panopea abrupta*, Conrad 1849) from 34 locations in British Columbia sampled between 1993 and 2000. Can. Tech. Rep. Fish. Aquat. Sci. 2413, 1–84.

Clark II, G.R., 1975. Periodic growth and biological rhythms in experimentally grown bivalves. In: Rosenberg, G.D., Runcorn, S.K. (Eds.), Growth Rhythms and the History of the Earth's Rotation. J. Wiley and Sons, New York, pp. 103–117.

Coan, E.V., Scott, P.V., Bernard, F.R., 2000. Bivalve Seashells of Western North America. Santa Barbara Museum of Natural History, Santa Barbara. 764 pp.

Craig, H., Gordon, L.I., 1965. Deuterium and oxygen 18 variations in the ocean and the marine atmosphere. In: Tongiorgi, E. (Ed.), Stable Isotopes in Oceanographic Studies and Paleotemperatures. Cons. Naz. di Rech., Spoleto, Italy, pp. 9–130.

Dettman, D.L., Lohmann, K.C., 1995. Microsampling carbonates for stable isotope and minor element analysis; physical separation of samples on a 20 micrometer scale. J. Sed. Res. 65, 566–569.

Dodge, R.E., Vaišnys, J.R., 1980. Skeletal growth chronologies of recent and fossil corals. In: Rhoads, D.C., Lutz, R.A. (Eds.), Skeletal Growth of Aquatic Organisms. Plenum, New York, pp. 493–517.

Elliot, M., deMenocal, P.B., Linsley, B.K., Howe, S.S., 2003. Environmental controls on the stable isotopic composition of *Mercenaria mercenaria*: potential application to paleoenvironmental studies. Geochem. Geophys. Geosyst. 4, 1–16.

Epstein, S., Mayeda, T., 1953. Variation of O18 content of waters from natural sources. Geochim. Cosmochim. Acta 4, 213–224.
Epstein, S., Buchsbaum, R., Lowenstam, H.A., Urey, H.C., 1953. Revised carbonate-water isotopic temperature scale. Bull. Geol. Soc. Am. 64, 1315–1326.
Fiebig, J., Schöne, B.R., Oschmann, W., 2005. High-precision oxygen and carbon isotope analysis of very small (10–30 μg) amounts of carbonates using continuous flow isotope ratio mass spectrometry. Rapid Commun. Mass. Spectrom. 19, 2355–2358.
Fritts, H.C., 1972. Tree-rings and climate. Sci. Am. 226, 93–100.
Gillikin, D.P., De Ridder, F., Ulens, H., Elskens, M., Keppens, E., Baeyens, W., Dehairs, F., 2005. Assessing the reproducibility and reliability of estuarine bivalve shells (*Saxidomus giganteus*) for sea surface temperature reconstruction: implications for paleoclimate studies. Palaeogeogr. Palaeoclimatol. Palaeoecol. 228, 70–85.
Goman, M., Ingram, B.L., Strom, A., 2007. Composition of stable isotopes in geoduck (*Panopea abrupta*) shells: a preliminary assessment of annual and seasonal paleoceanographic changes in the northeast Pacific. Quat. Int. 188, 117–125.
Goodwin, C.L., 1976. Observations on spawning and growth of subtidal geoducks (*Panope generosa*, Gould). Proc. Natl. Shellfish. Assoc. 65, 49–58.
Goodwin, C.L., 1977. The effects of season on visual and photographic assessment of subtidal geoduck clam (*Panope generosa*, Gould) populations. Veliger 20, 155–158.
Goodwin, C.L., Pease, B., 1989. Species profiles: life histories and environmental requirements of coastal fish and invertebrates (Pacific Northwest): Pacific geoduck clam. U.S. Fish. Wildl Serv. Biol. Rep. 82 (11.120), US Army Corps of Engineers, TR EL-82-4. 14 p. (available at http://www.nwrc.usgs.gov/wdb/pub/species_profiles/82_11-120.pdf).
Goodwin, D.H., Flessa, K.W., Schöne, B.R., Dettman, D.L., 2001. Cross-calibration of daily growth increments, stable isotope variation, and temperature in the Gulf of California bivalve mollusk *Chione cortezi*: implications for paleoenvironmental analysis. Palaios 16, 387–398.
Gribben, P.E., Creese, R.G., 2003. Protandry in the New Zealand geoduck, *Panopea zelandica* (Mollusca, Bivalvia). Invertebr. Reprod. Dev. 44, 119–129.
Grossman, E.L., Ku, T.-L., 1986. Oxygen and carbon isotope fractionation in biogenic aragonite; temperature effects. Chem. Geol. (Isotope Geoscience Section) 59, 59–74.
Henderson, J.T., 1929. Lethal temperatures of Lamellibranchiata. Contrib. Can. Biol. Fish. 4, 399–411.
Hudson, J.H., Shinn, E., Halley, R., Lidz, B., 1976. Sclerochronology: a new tool for interpreting past environments. Geology 4, 361–364.
Johnson, A.L.A., Hickson, J.A., Swan, J., Brown, M.R., Heaton, T.H.E., Chenery, S., Balson, P.S., 2000. The Queen Scallop *Aequipecten opercularis*: a new source of information on late Cenozoic marine environments in Europe. Geol. Soc. Spec. Publ. 177, 425–439.
Jones, D.S., 1980. Annual cycle of shell growth increment formation in two continental shelf bivalves and its paleoecologic significance. Paleobiology 6, 331–340.
Jones, D.S., Quitmyer, I.R., 1996. Marking time with bivalve shells: oxygen isotopes and season of annual increment formation. Palaios 11, 340–346.
Jones, D.S., Arthur, M.A., Allard, D.J., 1989. Sclerochronological records of temperature and growth from shells of *Mercenaria mercenaria* from Narragansett Bay, Rhode Island. Mar. Biol. 102, 225–234.
Kennish, M.J., Olsson, R.K., 1975. Effects of thermal discharges on the microstructural growth of *Mercenaria mercenaria*. Environ. Geol. (Springer) 1, 41–64.
Kurtzman, D., Scanlon, B.R., 2007. El Niño — Southern Oscillation and Pacific Decadal Oscillation impacts on precipitation in the southern and central United States: evaluation of spatial distribution and predictions. Water Resour. Res. 43, W10427. doi:10.1029/2007WR005863.
Mackas, D.L., Harrison, P.J., 1997. Nitrogenous nutrient sources and sinks in the Juan de Fuca Strait/Strait of Georgia/Puget Sound estuarine system: assessing the potential for eutrophication. Estuar. Coast. Shelf Sci. 44, 1–21.
Marchitto, T.A., Jones, G.A., Goodfriend, G.A., Weidman, C.R., 2000. Precise temporal correlation of Holocene mollusk shells using sclerochronology. Quat. Res. 53, 236–246.
Miyaji, T., Tanabe, K., Schöne, B.R., 2007. Environmental controls on daily shell growth of *Phacosoma japonicum* (Bivalvia: Veneridae) from Japan. Mar. Ecol. Prog. Ser. 336, 141–150.
Morsán, E., Ciocco, N.F., 2004. Age and growth model for the southern geoduck, *Panopea abbreviata*, off Puerto Lobos (Patagonia, Argentina). Fish. Res. 69, 343–348.
Nakaoka, M., 2000. Nonlethal effects of predators on prey populations: predator-mediated change in bivalve growth. Ecol. 81, 1031–1045.
Noakes, D.J., Campbell, A., 1992. Use of geoduck clams to indicate changes in the marine environment of Ladysmith Harbor, British Columbia. Environmetrics 3, 81–97.
O'Neil, J.R., Clayton, R.N., Mayeda, T.K., 1969. Oxygen isotope fractionation in divalent metal carbonates. J. Chem. Phys. 51, 5547–5558.
Page, H.M., Hubbard, D.M., 1987. Temporal and spatial patterns of growth in mussels *Mytilus edulis* on an offshore platform: relationships to water temperature and food availability. J. exp. Mar. Biol. Ecol. 111, 159–179.
Peterson, C.H., Quammen, M.L., 1982. Siphon nipping: its importance to small fishes and its impact on growth of the bivalve *Protothaca staminea* (Conrad). J. Exp. Mar. Biol. Ecol. 63, 249–268.
Rodland, D.L., Schöne, B.R., Helama, S., Nielsen, J.K., Baier, S., 2006. A clockwork mollusc: ultradian rhythms in bivalve activity revealed by digital photography. J. Exp. Mar. Bio. Ecol. 334, 316–323.
Sato, S., 1997. Shell microgrowth patterns of bivalves reflecting seasonal change of phytoplankton abundance. Paleontol Res 1, 260–266.
Schöne, B.R., Oschmann, W., Rössler, J., Freyre Castro, A.D., Houk, S.D., Kröncke, I., Dreyer, W., Janssen, R., Rumohr, H., Dunca, E., 2003. North Atlantic Oscillation dynamics recorded in shells of a long-lived bivalve mollusk. Geology 31, 1237–1240.
Schöne, B.R., Castro, A., Fiebig, J., Houk, S., Oschmann, W., Kroncke, I., 2004a. Sea surface temperatures over the period 1884–1983 reconstructed from oxygen isotope ratios of a bivalve mollusk shell (*Arctica islandica*, southern North Sea). Palaeogeogr. Palaeoclimatol. Palaeoecol. 212, 215–232.
Schöne, B.R., Dunca, E., Mutvei, H., Norlund, U., 2004b. A 217-year record of summer air temperature reconstructed from freshwater pearl mussels (*M. margarifitera*, Sweden). Quat. Sci. Rev. 23, 1803–1816 + 2057.
Schöne, B.R., Fiebig, J., Pfeiffer, M., Gleß, R., Hickson, J., Johnson, A.L.A., Dreyer, W., Oschmann, W., 2005a. Climate records from a bivalve Methuselah (*Arctica islandica*, Mollusca; Iceland). Palaeogeogr. Palaeoclimatol. Palaeoecol. 228, 130–148.
Schöne, B.R., Pfeiffer, M., Pohlmann, T., Siegismund, F., 2005b. A seasonally resolved bottom-water temperature record fort he period AD 1866–2002 based on shells of *Arctica islandica* (Mollusca, North Sea). Int. J. Climatol. 25, 947–962.
Schöne, B.R., Dunca, E., Fiebig, J., Pfeiffer, M., 2005c. Mutvei's solution: an ideal agent for resolving microgrowth structures of biogenic carbonates. Palaeogeogr. Palaeoclimatol. Palaeoecol. 228, 149–166.
Schöne, B.R., Rodland, D.L., Fiebig, J., Oschmann, W., Goodwin, D., Flessa, K.W., Dettman, D., 2006. Reliability of multitaxon, multiproxy reconstructions of environmental conditions from accretionary biogenic skeletons. J. Geol. 114, 267–285.
Shaul, W., Goodwin, L., 1982. Geoduck (*Panope generosa*: Bivalvia) age as determined by internal growth lines in the shell. Can. J. Fish. Aquat. Sci. 39, 632–636.
Spötl, C., Vennemann, T.W., 2003. Continuous-flow isotope ratio mass spectrometric analysis of carbonate minerals. Rapid Commun. Mass. Spectrom. 17, 1004–1006.
Strom, A., Francis, R.C., Mantua, N.J., Miles, E.L., Peterson, D.L., 2004. North Pacific climate recorded in growth rings of geoduck clams: a new tool for paleoenvironmental reconstruction. Geophys. Res. Lett. 31, L06206. doi:10.1029/2004GL019440.
Strom, A., Francis, R.C., Mantua, N.J., Miles, E.L., Peterson, D.L., 2005. Preserving low-frequency climate signals in growth records of geoduck clams (*Panopea abrupta*). Palaeogeogr. Palaeoclimatol. Palaeoecol. 228, 167–178.
Surge, D., Walker, K.J., 2006. Geochemical variation in microstructural shell layers of the southern quahog (*Mercenaria campechiensis*): implications for reconstructing seasonality. Palaeogeogr. Palaeoclimatol. Palaeoecol. 237, 182–190.
Urey, H.C., Lowenstam, H.A., Epstein, S., McKinney, C.R., 1951. Measurement of paleotemperatures and temperatures of the Upper Cretaceous of England, Denmark, and the southeastern United States. Bull. Geol. Soc. Am. 62, 399–416.
Walker, G.T., 1923. Correlation in seasonal variations of weather, VIII: a preliminary study of world weather. Mem. Ind. Meteorol. Dept. 24, 75–131.
Wanamaker Jr., A.D., Kreutz, K.J., Schöne, B.R., Pettigrew, N., Borns, H.W., Introne, D.S., Belknap, D., Maasch, K.A., Feindel, S., 2007. Coupled North Atlantic slope water forcing on Gulf of Maine temperatures over the past millennium. Clim. Dyn. 31, 183–194.
Weiner, S., Dove, P.M., 2003. An overview of biomineralization processes and the problem of the vital effect. In: Dove, P.M., DeYoreo, J.J., Weiner, S. (Eds.), Biomineralization. Rev. Min. Geochem., vol. 54, pp. 1–29.
Zolotarev, V.N., 1980. The life span of bivalves from the Sea of Japan and Sea of Okhotsk. Soviet J. Mar. Biol. 6, 301–308.